Preparation and Structural Characterization of $Mo_2Cl_4(OAc)_2(PR_3)_2$ Compounds (R = Me, Et) and a Comparative Study of the Singlet–Triplet Separation for $Mo_2Cl_4(OAc)_2(PEt_3)_2$ with That for $Mo_2Cl_6(dppm)_2$

F. Albert Cotton,* Jianrui Su, Zhong Sheng Sun, and Hong Chen

Department of Chemistry and Laboratory for Molecular Structure and Bonding, Texas A&M University, College Station, Texas 77843

*Received March 30, 1993**

Two new compounds $Mo_2Cl_4(OAc)_2(PEt_3)_2$ (**1**) and $Mo_2Cl_4(OAc)_2(PMe_3)_2$ (**2**) have been synthesized and found to be paramagnetic. Their structures were determined by X-ray crystallography, and the proton NMR spectrum of compound **1** was recorded as a function of temperature in order to evaluate its singlet–triplet energy gap; this was found to be 1033 ± 5 cm^{-1}. It is interesting to find that compound **1**, compared with $Mo_2Cl_6(dppm)_2$[1,2] **3**, has the shorter Mo–Mo distance but the smaller singlet–triplet energy gap. The reason for this is discussed. The crystallographic data for these compounds are as follows: **1**, orthorhombic $Pca2_1$ with a = 7.494(0) Å, b = 15.863(3) Å, c = 22.622(2) Å, V = 2689(2) Å^3, Z = 4, R = 0.033, and R_w = 0.044; **2**, monoclinic $P2_1/c$ with a = 6.616(2) Å, b = 10.308(2) Å, c = 16.593(2) Å, β = 91.19(1)°, V = 1131.4(7) Å^3, Z = 2, R = 0.060, and R_w = 0.076.

Introduction

Many edge-sharing bioctahedral (ESBO) dinuclear metal compounds have been synthesized and well characterized,[1-3] but d^3–d^3 ESBO systems remain especially interesting due to the uncertainty of their bond order and bonding scheme. There are a number of factors that influence the metal–metal bonding, for which the main indices have been the M–M distance and the singlet–triplet energy gap. The basicity of the bridging and the terminal ligands,[2] the π-donating ability of bridging atoms,[3] and the nature of bridging bidentate ligands such as carboxylate groups, as well as steric factors, could all have a significant effect on the M–M bonding.

It is well-known that, solely on the basis of metal–metal overlaps, we should find the following energy level ordering:

$$\sigma \ll \pi < \delta < \delta^* < \pi^* \ll \sigma^*$$

In a molecule, however, the actual metal–metal bonding orbitals have contributions from ligand orbitals; i.e., the ordering is influenced by coordination with ligands, and as a result, the actual energy level ordering may not be the same as that expected from "pure" metal–metal interactions.

Shaik and Hoffmann carried out molecular orbital calculations on a series of d^3–d^3 ESBO compounds possessing D_{2h} symmetry, e.g. $Mo_2Cl_6(dppm)_2$ (**3**) (dppm = bis(diphenylphosphino)-methane) in 1980 and found that mixing into the δ orbital of p orbitals on the bridging chlorine atoms pushes the δ orbital up in energy while there is no similar effect for δ^*. This results in a smaller δ–δ^* energy gap or even in a reversal of the δ–δ^* energy level ordering.[3]

Similarly, if the dppm ligands in compound **3** are replaced by carboxylate or formamidinate groups, which contain occupied nonbonding π orbitals, the possible mixing of δ and δ^* with the pπ ligand orbitals should be taken into account.

We have begun a systematic study designed to synthesize sets of compounds in which only one of the aforementioned factors is changed at one time. Some interesting preliminary results have already been obtained.

Experimental Section

General Procedures. All manipulations were carried out under an atmosphere of nitrogen unless otherwise specified. Standard Schlenk and vacuum-line techniques were used. Tetrahydrofuran, hexanes, and benzene were dried over and freshly distilled from potassium/sodium benzophenone ketyl, and ethanol was distilled from magnesium prior to use. Phosphines were purchased from Strem Chemicals and used as received. Anhydrous sodium acetate was used as purchased. Potassium acetate was distilled in ethanol and benzene in sequence to remove moisture and then dried in vacuum. $MoCl_3(THF)_3$ and $Mo_2Cl_6(THF)_3$ were prepared by literature methods[4,5] and dried in vacuum prior to use. ^1H NMR (200 MHz) spectra were recorded on a Varian XL-200 spectrometer.

Preparation of $Mo_2Cl_4(OAc)_2(PEt_3)_2$ (1). A mixture of 0.50 g of $Mo_2Cl_6(THF)_3$ (0.81 mmol) and an excess of previously dried potassium acetate (1.0 g, 10.2 mmol) was stirred in 20 mL of THF for 20 min before 0.15 mL (0.12 g, 1.0 mmol) of PEt_3 was added. A dark brown-red solution was obtained after the mixture had been stirred for 24 h at room temperature. The solution was filtered, and the filtrate was directly layered with hexanes in a Schlenk tube. Brown-orange crystals were obtained after 20 days of diffusion. The supernatant liquid, which was still very dark, was transferred through a cannula and discarded. The crystals were washed with a mixture of benzene and hexanes and dried in vacuum (0.22 g, 40%).

Preparation of $Mo_2Cl_4(OAc)_2(PMe_3)_2$ (2). A mixture of 0.50 g of $MoCl_3(THF)_3$ (1.19 mmol) and an excess of sodium acetate (1.0 g, 12 mmol) was stirred in 20 mL of THF for 20 min before 0.14 mL (0.12 g, 1.55 mmol) of PMe_3 was added. A black-brown solution was obtained after the mixture had been stirred for 10 h at room temperature. The solution was filtered, and the filtrate was directly layered with hexanes in a Schlenk tube. After diffusion was complete, the solution was allowed to stand for another 10 days. Orange crystals which formed near the top of the solution were picked manually and washed with hexanes (0.047 g, 6.5%).

Electronic Spectroscopy. The electronic spectrum of compound **1** was obtained on a Cary 17 spectrophotometer. It is shown in Figure 1. The principal features are absorptions at 403 and 510 nm.

* Abstract published in *Advance ACS Abstracts*, September 15, 1993.

(1) Chakravarty, A. R.; Cotton, F. A.; Diebold, M. P.; Lewis, D. B.; Roth, W. J. *J. Am. Chem. Soc.* **1986**, *108*, 971.
(2) Cotton, F. A.; Eglin, J. L.; James, C. A.; Luck, R. L. *Inorg. Chem.* **1992**, *31*, 5308.
(3) Shaik, S.; Hoffmann, R.; Fisel, C. R.; Summerville, R. H. *J. Am. Chem. Soc.* **1980**, *102*, 4555.
(4) (a) Dilworth, J. R.; Richards, R. L. *Inorg. Synth.* **1980**, *20*, 121. (b) Dilworth, J. R.; Zubieta, J. *Inorg. Synth.* **1986**, *24*, 193.
(5) Boyd, I. W.; Wedd, A. G. *Aust. J. Chem.* **1976**, *29*, 1829.
(6) (a) Campbell, G. C.; Haw, J. F. *Inorg. Chem.* **1988**, *27*, 3706. (b) Boersma, A. D.; Phillippi, M. A.; Goff, H. M. *J. Magn. Reson.* **1984**, *57*, 197. (c) La Mar, G. N.; Horrocks, W. D., Jr.; Holm, R. H. *NMR of Paramagnetic Molecules*; Academic Press: New York and London, 1973, Chapter 7.

0020-1669/93/1332-4871$04.00/0

Figure 1. Electronic spectrum of compound **1**.

IR Spectroscopy. The IR spectrum of compound **1** was recorded on a Perkin-Elmer 783 spectrophotometer. The observed absorption peaks of compound **1** (Nujol mull, KBr plates) were at 215 (m), 225 (w), 250 (w), 275 (w), 290 (w), 300 (w), 665 (w), 720 (m), 1360 (s), 1445 (s), 2330 (w), 2820 (s), and 2890 (s) cm^{-1}.

X-ray Crystallography. The single-crystal diffraction experiments were conducted using an Enraf-Nonius CAD-4 diffractometer with Mo Kα radiation and an AFC5R Rigaku with Cu Kα radiation for compounds **1** and **2**, respectively. Lattice dimensions and Laue symmetry were verified using axial photographs. Three standard reflections were measured every hour during data collections to monitor any gain or loss in intensity. Corrections, which would have been applied if ΔI had been greater than 5%, were not required. The absorption corrections were applied by employing the empirical ψ-scan method based on the azimuthal scans of several reflections with diffractometer angle χ near 90°. Data reduction was carried out by standard methods with the use of well-established computational procedures, and crystallographic computing was done on a local area VAX cluster, employing the VAX/VMS V5.4 computer and Enraf-Nonius SDP software. Because both compounds **1** and **2** are fairly stable, no special precautions were taken in mounting the crystals and collecting the data. The crystals were mounted on the top of thin glass fibers with epoxy cement. Basic information pertaining to the crystal parameters and the structure refinement are summarized in Table I. The positional parameters and equivalent isotropic thermal displacement parameters for non-hydrogen atoms are listed in Table II, and the principal bond lengths and angles are given in Table III.

The coordinates of the two crystallographically independent molybdenum atoms in **1** were obtained by the Patterson method (SHELXS-86) in the standard space group $Pca2_1$ (No. 29), which was later fully confirmed (as against *Pbcm*, No. 51, which is also consistent with the observed systematic absences) by the successful location of other non-hydrogen atoms and the refinement of the structure. The configuration of the molecule, which constitutes the asymmetric unit, is shown in Figure 2. When the other enantiomorph was refined, the R value decreased from 0.033 47 to 0.033 33; therefore the second enantiomorph was kept.

For compound **2**, the space group was uniquely assigned as $P2_1/c$ (No. 14) according to the systematic absences. The molecules were located on inversion centers with only a half molecule constituting the asymmetric unit. The coordinates of the molybdenum atoms were obtained by the Patterson method (SHELXS-86). Difference Fourier maps based on the refined positions of the molybdenum atoms revealed the positions of the remaining non-hydrogen atoms. These atoms were refined anisotropically in the final least-squares refinement. An ORTEP drawing of a molecule of compound **2** is presented in Figure 3. More information

Table I. Crystal Data for Compounds **1** and **2**

	$Mo_2Cl_4(OAc)_2(PEt_3)_2$ (**1**)	$Mo_2Cl_4(OAc)_2(PMe_3)_2$ (**2**)
formula	$C_{16}H_{36}Cl_4Mo_2O_4P_2$	$C_{10}H_{24}Cl_4Mo_2O_4P_2$
fw	688.10	603.94
space group	$Pca2_1$	$P2_1/c$
a, Å	7.494(2)	6.616(2)
b, Å	15.863(3)	10.308(2)
c, Å	22.622(7)	16.593(2)
β, deg	90	91.19(1)
V, Å^3	2689(2)	1131.4(7)
Z	4	2
d_{calc}, g/cm^3	1.54	1.58
μ, cm^{-1}	14.48	152.233
radiation (monochromated in incident beam)	Mo Kα (λ = 0.710 73 Å)	Cu Kα (λ = 1.541 78 Å)
temp, °C	20	20
transm factors: max, min	0.998, 0.827	1.000, 0.358
R^a	0.033 33	0.059 95
R_w^b	0.044 49	0.075 75

$^a R = \Sigma||F_o| - |F_c||/\Sigma|F_o|$. $^b R_w = [\Sigma w(|F_o| - |F_c|)^2/\Sigma w|F_o|^2]^{1/2}$; $w = 1/\sigma^2(|F_o|)$.

Table II. Positional and Equivalent Isotropic Thermal Parameters for $Mo_2Cl_4(OAc)_2(PEt_3)_2$

atom	x	y	z	B,^{a} Å^2
Mo(1)	0.90585(4)	0.77731(9)	1.000	1.78(1)
Mo(2)	0.84298(4)	0.79571(1)	0.86216(6)	1.81(1)
Cl(1)	0.9230(1)	0.9991(3)	0.8935(2)	2.72(5)
Cl(2)	0.8263(1)	0.5744(3)	0.9695(2)	2.77(5)
Cl(3)	0.9165(1)	0.5905(3)	1.1236(2)	2.88(5)
Cl(4)	0.8323(1)	0.9814(3)	0.7382(2)	2.84(5)
P(1)	0.9917(1)	0.9434(3)	1.0709(2)	2.15(5)
P(2)	0.7573(1)	0.6274(3)	0.7915(2)	2.25(5)
O(1)	0.9595(3)	0.6065(8)	0.9300(4)	2.5(1)
O(2)	0.9064(3)	0.6271(9)	0.8110(4)	2.4(1)
O(3)	0.8425(3)	0.9487(9)	1.0497(4)	2.6(1)
O(4)	0.7881(3)	0.9638(9)	0.9315(4)	2.3(1)
C(1)	0.9493(5)	0.566(1)	0.8543(7)	2.9(2)
C(2)	0.9917(6)	0.438(2)	0.8110(8)	4.2(3)
C(3)	0.7972(5)	1.006(1)	1.0088(6)	2.4(2)
C(4)	0.7572(5)	1.134(2)	1.0511(7)	3.9(2)
C(5)	1.0114(5)	1.162(1)	1.0296(7)	3.1(2)
C(6)	1.0615(6)	1.258(1)	1.0765(9)	4.2(3)
C(7)	0.9822(5)	0.977(1)	1.1848(6)	2.9(2)
C(8)	0.9313(6)	1.102(2)	1.2091(8)	4.0(3)
C(9)	1.0610(5)	0.811(1)	1.0668(7)	3.0(2)
C(10)	1.0866(5)	0.798(2)	0.9788(9)	4.3(3)
C(11)	0.6877(6)	0.754(2)	0.7979(9)	4.7(3)
C(12)	0.6604(7)	0.748(2)	0.885(1)	6.6(4)
C(13)	0.7418(5)	0.400(1)	0.8310(7)	3.0(2)
C(14)	0.6919(6)	0.303(2)	0.7862(8)	4.0(3)
C(15)	0.7642(6)	0.600(1)	0.6760(6)	3.7(3)
C(16)	0.8179(6)	0.484(2)	0.6532(7)	5.1(3)

^{a} Anisotropically refined atoms are given in the form of the isotropic equivalent displacement parameter defined as $(4/3)[a^2B(1,1) + b^2B(2,2) + c^2B(3,3) + ab(\cos\gamma)B(1,2) + ac(\cos\beta)B(1,3) + bc(\cos\alpha)B(2,3)]$.

concerning the crystal parameters and structure refinement of **2** are summarized in Table I. The positional parameters and selected bond distances and angles are presented in Tables IV and V, respectively.

^{1}H NMR Analysis. The following equation describes the variation of the NMR chemical shifts with temperature in a system with a singlet ground state and a triplet excited state:[6]

$$H_{obsd} = H_{dia} + \frac{2g\beta H_0 A}{(\gamma/2\pi)kT}(3 + e^{2J/kT})^{-1} \quad (1)$$

In this equation H_{obsd} is the resonance position of the proton under study, H_{dia} is the resonance position that the same nucleus would have in an equivalent diamagnetic environment, T is the absolute temperature, γ is the gyromagnetic ratio of the nucleus, H_0 is the resonance position of the nucleus, g and β are the Landé splitting factor and Bohr magneton for an electron, and A is the hyperfine coupling constant between the electron and nucleus concerned. On the assumption of a negligible dipolar contribution, the singlet state–triplet state energy level splitting, $-2J$

Table III. Selected Bond Distances (Å) and Angles (deg) for $Mo_2Cl_4(OAc)_2(PEt_3)_2$[a]

Distances			
Mo(1)–Mo(2)	2.612(1)	Mo(2)–O(4)	2.083(6)
Mo(1)–Cl(1)	2.402(3)	P(1)–C(5)	1.82(1)
Mo(1)–Cl(2)	2.406(3)	P(2)–C(11)	1.84(1)
Mo(1)–Cl(3)	2.421(3)	P(2)–C(13)	1.85(1)
Mo(1)–P(1)	2.567(3)	P(2)–C(15)	1.85(1)
Mo(1)–O(1)	2.085(7)	O(1)–C(1)	1.26(1)
Mo(1)–O(3)	2.079(7)	O(2)–C(1)	1.27(1)
Mo(2)–Cl(1)	2.418(3)	O(3)–C(3)	1.29(1)
Mo(2)–Cl(2)	2.407(3)	O(4)–C(3)	1.28(1)
Mo(2)–Cl(4)	2.421(3)	C(1)–C(2)	1.52(2)
Mo(2)–P(2)	2.569(3)	C(3)–C(4)	1.48(2)
Mo(2)–O(2)	2.077(7)		

Angles			
Mo(2)–Mo(1)–Cl(3)	139.68(7)	Mo(1)–Cl(1)–Mo(2)	65.63(7)
Mo(2)–Mo(1)–P(1)	138.88(6)	Mo(1)–Cl(2)–Mo(2)	65.74(7)
Mo(2)–Mo(1)–O(1)	84.5(2)	Mo(1)–P(1)–C(5)	117.7(4)
Mo(2)–Mo(1)–O(3)	84.8(2)	Mo(1)–P(1)–C(7)	114.1(4)
Cl(1)–Mo(1)–Cl(2)	114.62(9)	Mo(1)–P(1)–C(9)	111.4(3)
Cl(3)–Mo(1)–P(1)	81.39(8)	C(5)–P(1)–C(7)	105.0(5)
P(1)–Mo(1)–O(1)	95.2(2)	Mo(2)–P(2)–C(11)	111.6(4)
P(1)–Mo(1)–O(3)	93.2(2)	C(11)–P(2)–C(13)	107.1(6)
O(1)–Mo(1)–O(3)	169.3(3)	Mo(1)–O(1)–C(1)	123.3(6)
Mo(1)–Mo(2)–Cl(4)	139.88(7)	Mo(2)–O(2)–C(1)	122.2(6)
Mo(1)–Mo(2)–P(2)	138.57(7)	Mo(1)–O(3)–C(3)	124.3(6)
Mo(1)–Mo(2)–O(2)	85.4(2)	Mo(2)–O(4)–C(3)	123.9(6)
Mo(1)–Mo(2)–O(4)	85.1(2)	O(1)–C(1)–O(2)	124.6(9)
Cl(1)–Mo(2)–Cl(2)	114.01(9)	O(3)–C(3)–O(4)	121.9(9)
Cl(4)–Mo(2)–P(2)	81.52(9)		

[a] Numbers in parentheses are estimated standard deviations in the least significant digits.

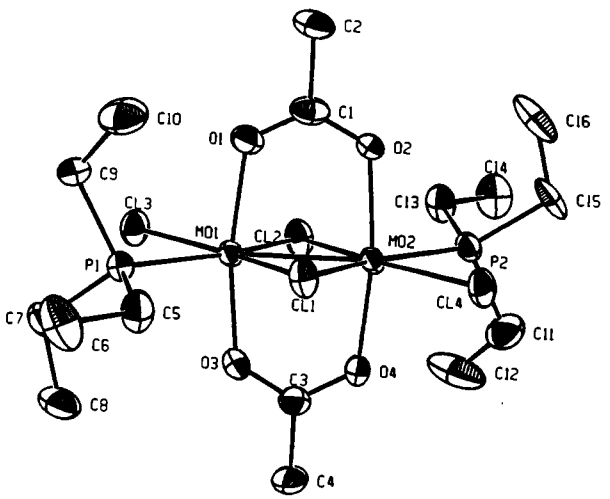

Figure 2. ORTEP drawing of compound **1**. The thermal ellipsoids are drawn at 50% probability.

(from the spin Hamiltonian $H = -2JS_1 \cdot S_2$), H_{dia}, and A values can be calculated by using a multiple-parameter, nonlinear least-squares procedure to fit the variable-temperature data to eq 1. This method has been used previously.[2,7,8] It is also assumed in using eq 1 that most of the molecules are in the ground state ($S = 0$, singlet state), while the percentage of the molecules with higher energy than the first excited state ($S = 1$, triplet state) is so small that the contribution of these molecules is negligible. Therefore only the molecules in the first excited state are assumed to be responsible for the weak paramagnetism and hence for the anomalous chemical shifts in the variable-temperature NMR spectra.

Results and Discussion

We recognize that the preparative methods employed for the two new compounds reported here are not very efficient. Attempts to increase the yields by obvious changes such as increasing time of reaction, refluxing, or employing other solvents have not been successful. Real improvement will probably require the use of

(7) Cotton, F. A.; Eglin, J. L.; Hong, B.; James, C. A. *J. Am. Chem. Soc.* **1992**, *114*, 4915.
(8) Cotton, F. A.; Chen, H.; Daniels, L. M.; Feng, X. *J. Am. Chem. Soc.* **1992**, *114*, 8980.

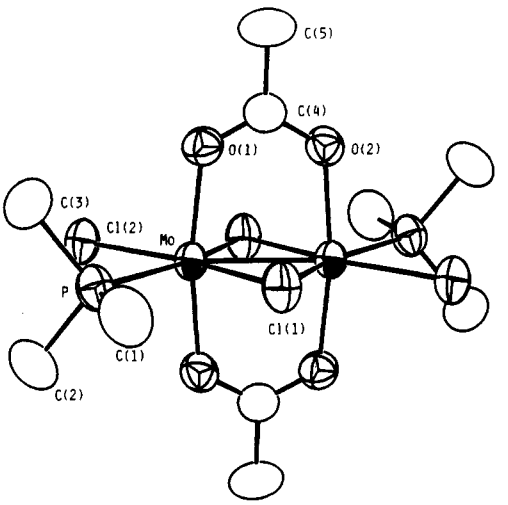

Figure 3. ORTEP drawing of compound **2**. The thermal ellipsoids are drawn at 50% probability.

Table IV. Positional and Equivalent Isotropic Thermal Parameters for $Mo_2Cl_4(OAc)_2(PMe_3)_2$

atom	*x*	*y*	*z*	B,[a] Å^2
Mo	0.53477(7)	0.56277(4)	0.56657(3)	3.13(1)
Cl(1)	0.2522(2)	0.6106(2)	0.4790(1)	4.30(3)
Cl(2)	0.7719(3)	0.5658(2)	0.6802(1)	4.57(4)
P	0.3863(3)	0.7512(2)	0.6451(1)	4.10(3)
O(1)	0.3538(7)	0.4215(4)	0.6195(3)	4.1(1)
O(2)	0.2952(7)	0.3130(4)	0.5045(3)	3.98(9)
C(1)	0.163(1)	0.8337(8)	0.6070(6)	6.2(2)
C(2)	0.571(1)	0.8772(8)	0.6606(7)	6.3(2)
C(3)	0.316(1)	0.7055(9)	0.7480(5)	5.9(2)
C(4)	0.2721(9)	0.3293(6)	0.5798(4)	3.8(1)
C(5)	0.144(1)	0.2346(9)	0.6227(6)	6.7(2)

[a] Anisotropically refined atoms are given in the form of the isotropic equivalent displacement parameter defined as $(4/3)[a^2B(1,1) + b^2B(2,2) + c^2B(3,3) + ab(\cos\gamma)B(1,2) + ac(\cos\beta)B(1,3) + bc(\cos\alpha)B(2,3)]$.

Table V. Selected Bond Distances (Å) and Bond Angles (deg) for $Mo_2Cl_4(OAc)_2(PMe_3)_2$[a]

Distances			
Mo–Mo	2.5932(7)	P–C(1)	1.808(9)
Mo–Cl(1)	2.395(2)	P–C(2)	1.797(9)
Mo–Cl(1)	2.407(2)	P–C(3)	1.841(9)
Mo–Cl(2)	2.427(2)	O(1)–C(4)	1.271(8)
Mo–P	2.547(2)	O(2)–C(4)	1.273(9)
Mo–O(1)	2.091(5)	C(4)–C(5)	1.49(1)
Mo–O(2)	2.086(4)		

Angles			
Mo–Mo–Cl(1)	57.54(4)	Cl(2)–Mo–O(2)	94.8(1)
Mo–Mo–Cl(1)	57.10(4)	P–Mo–O(1)	94.9(1)
Mo–Mo–Cl(2)	140.21(5)	P–Mo–O(2)	92.3(1)
Mo–Mo–P	138.83(4)	O(1)–Mo–O(2)	170.3(2)
Mo–Mo–O(1)	85.3(1)	Mo–Cl(1)–Mo	65.36(4)
Mo–Mo–O(2)	85.0(1)	Mo–P–C(1)	120.1(3)
Cl(1)–Mo–Cl(1)	114.64(6)	Mo–P–C(2)	110.9(3)
Cl(1)–Mo–Cl(2)	162.21(6)	Mo–P–C(3)	112.8(3)
Cl(1)–Mo–P	81.32(6)	C(1)–P–C(2)	104.9(4)
Cl(1)–Mo–O(1)	87.2(1)	C(1)–P–C(3)	102.9(4)
Cl(1)–Mo–O(2)	87.4(1)	C(2)–P–C(3)	103.7(5)
Cl(1)–Mo–Cl(2)	83.12(6)	Mo–O(1)–C(4)	122.9(5)
Cl(1)–Mo–P	163.97(6)	Mo–O(2)–C(4)	123.4(4)
Cl(1)–Mo–O(1)	87.7(1)	O(1)–C(4)–O(2)	123.4(6)
Cl(1)–Mo–O(2)	87.3(1)	O(1)–C(4)–C(5)	118.9(7)
Cl(2)–Mo–P	80.95(6)	O(2)–C(4)–C(5)	117.8(6)
Cl(2)–Mo–O(1)	92.8(1)		

[a] Numbers in parentheses are estimated standard deviations in the least significant digits.

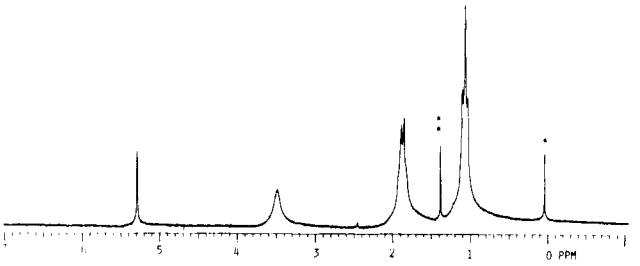

Figure 4. ^1H NMR spectrum of $Mo_2Cl_4(OAc)_2(PEt_3)_2$ (**1**) in CD_2Cl_2 at 25 °C. Single and double asterisks denote peaks of grease and other impurities.

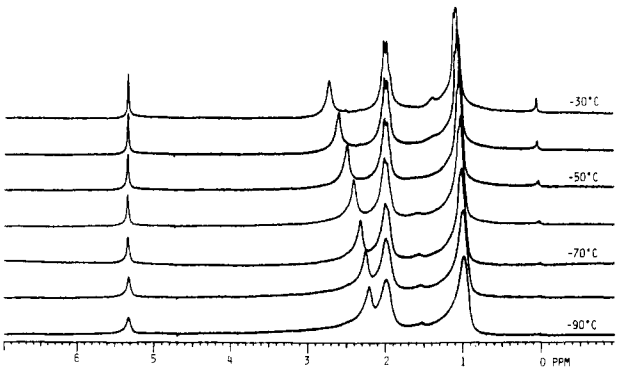

Figure 5. Part of the variable-temperature ^1H NMR spectra of $Mo_2Cl_4(OAc)_2(PEt_3)_2$ (**1**) in CD_2Cl_2.

different starting materials, and this is now under study. However, we present this report because the behavior of the compounds presents features of sufficient interest to make the inefficient preparations tolerable, at least *pro tem*.

$Mo_2Cl_4(OAc)_2(PEt_3)_2$ (**1**) was found to be weakly paramagnetic, to the extent that no signal was detected in its $^{31}P\{^1H\}$ NMR spectra at ambient temperature, although the Mo–Mo distance in the molecule is only 2.61 Å.

The ^1H NMR spectra of compound **1**, recorded on a Varian XL-200 spectrometer in CD_2Cl_2 in the widest possible temperature range (from −90 to +30 °C) at 10 °C intervals and a preacquisition delay of 10 min, are shown in Figures 4 and 5. The peaks at δ 0 and 1.4 ppm were caused by grease and other impurities, while the one at δ 5.3 ppm is due to residual ^1H in the CD_2Cl_2. The integrations of the other three peaks in the spectrum at 25 °C (Figure 4) are 11.5, 22.7, and 34.8 from left to right, which allows them to be assigned unambiguously to the $-CH_3$ groups in the acetate ligands and to the $-CH_2-$ and the $-CH_3$ groups in the triethylphosphines, respectively. It is obvious from the spectra in Figure 5 that the signals for protons in the acetate groups are shifted the most while those for protons in the phosphine ligands are shifted rather little as the temperature changes. Our calculations of the singlet–triplet gap ($-2J$) of compound **1** were therefore based on the chemical shift of the signals of the acetate protons. The data are plotted in Figure 6.

It should be noted that the singlet–triplet gap for compound **3** was obtained using the same calculation method but from $^{31}P\{^1H\}$ NMR. However, compound **1** is obviously more paramagnetic than compound **3** simply on the basis of the fact that the $^{31}P\{^1H\}$ NMR spectrum was not observed for compound **1**. This is consistent with the result that compound **1** has a smaller singlet–triplet gap than compound **3**.

It might have been expected that a shorter metal–metal distance would result in a greater singlet–triplet splitting, because of a larger HOMO (δ or δ^*)–LUMO (δ^* or δ) energy gap. However, this need not be the case, as shown in Table VI by the comparison of compound **1** with compound **3**. We must now seek an explanation for this in terms of the major difference between molecules **1** and **3**, namely, the presence of two acetate groups in the axial positions of **1** instead of two dppm ligands in **3**.

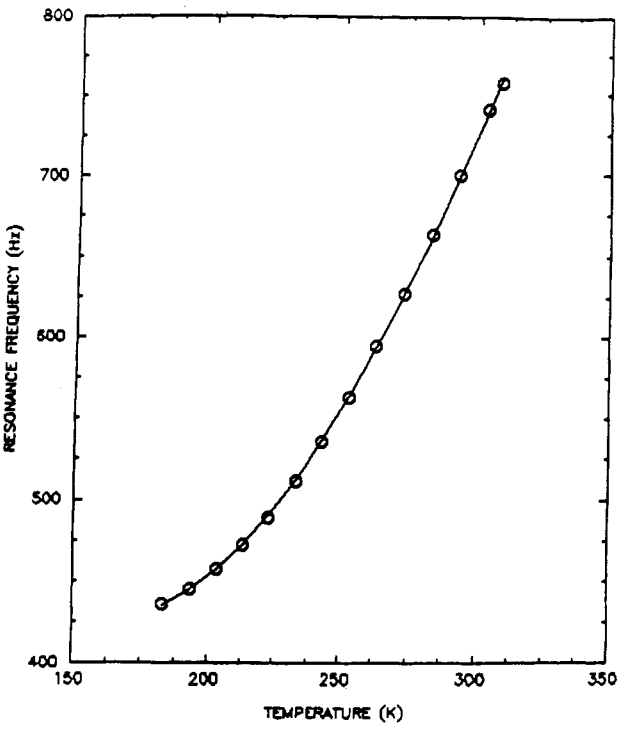

Figure 6. Plot of the temperature-dependent chemical shifts of CH_3 protons in acetate ligands versus temperature for $Mo_2Cl_4(OAc)_2(PEt_3)_2$ (**1**), with H_{dia} = 412.66 Hz, A = 1.07 MHz, and $-2J$ = 1033 ± 5 cm^{-1}.

Table VI. Comparison of $Mo_2Cl_4(OAc)_2(PEt_3)_2$ (**1**) with $Mo_2Cl_6(dppm)_2$ (**3**)

	1	**2**
Mo–Mo, Å	2.61	2.79
Mo–(μ-Cl)–Mo, deg	65.7	70.9
singlet–triplet gap with estd errors, cm^{-1}	1033 ± 5	1460 ± 30

Compound **2** has imposed symmetry of C_{2h} while compound **1** does not. But compound **1** can be considered as having effective C_{2h} symmetry if the ethyl groups on the phosphorus atoms are considered to be rotating about the Mo–P bond. The C_2 axis is defined by the two C–C bonds of the acetate groups. Although there is no C_2 symmetry element along the Mo–Mo axis, the four Mo–(μ-Cl) distances in both compounds **1** and **2** are virtually the same, as shown in Tables III and V. This indicates that the equatorial phosphines in compounds **1** and **2**, which do not exist in compound **3**, do not help to make the coordination environments around molybdenum atoms in compounds **1** and **2** very different from that in compound **3**. Compared with those of compound **3**, the same Mo–(μ-Cl) distances but considerably shorter Mo–Mo distances in compounds **1** and **2** result in a smaller Mo–(μ-Cl)–Mo angle, which gives rise to a better overlap of the p orbital of the bridging chlorine atoms with the δ orbital and thus should tend to push the δ orbital even higher in energy, as shown in Figure 7. While the other combination of the two bridging chlorine p orbitals has the same symmetry species (i.e., a_u) as the δ^* orbital in the C_{2h} point group, they are virtually orthogonal and thus their overlap is essentially nil. The interaction is therefore negligible.

While, in compound **3**, the interaction of the δ orbital with the μ-Cl pπ orbitals is the only important ligand influence on the δ–δ^* gap, there is an additional interaction in the case of compounds of type **1** and **2**. As shown in Figure 8, the bridging carboxylate groups have π orbitals spanning their CO_2 moieties. In each carboxylate group there is a strongly bonding π orbital that contains two electrons; the energy of this orbital is expected to be considerably lower than the energies of the δ and δ^* orbitals. Also present on each carboxylate group is an empty π^* orbital

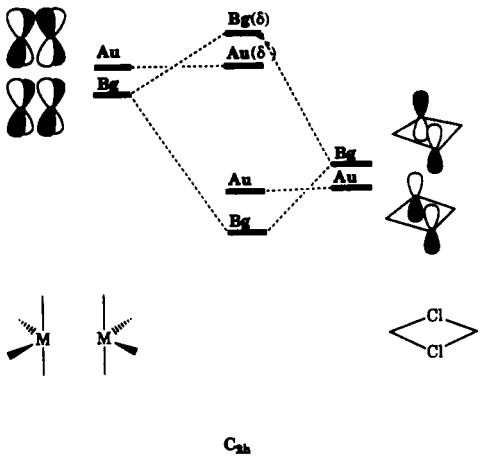

C_{2h}

Figure 7. Interaction of the metal δ orbitals with the π orbitals on the bridging chlorine atoms.

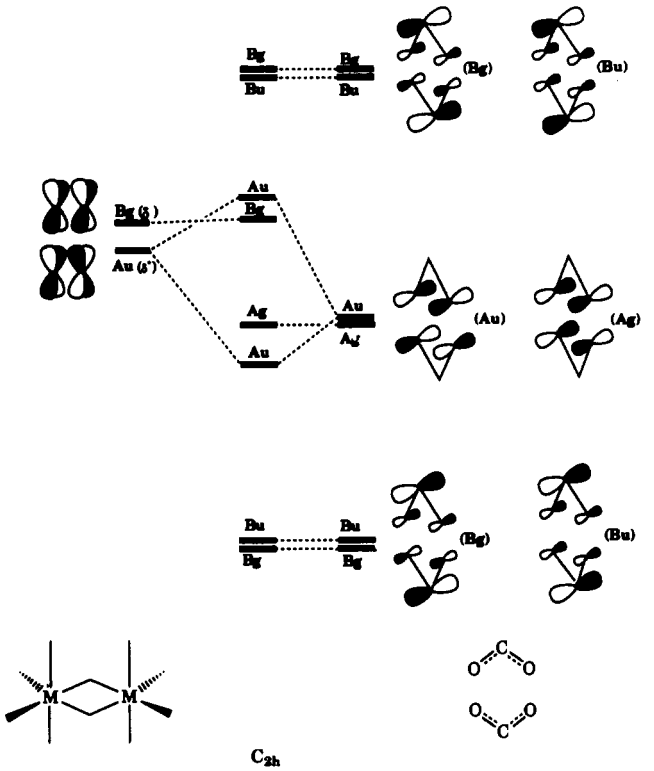

C_{2h}

Figure 8. Interaction of the metal δ^* orbitals with the π orbitals on the bridging acetate ligands.

that is expected to be at much higher energy than the δ and δ^* orbitals. The important interaction between the carboxylate groups and the δ and δ^* orbitals will be caused by the middle π orbital of each carboxylate group, which is filled, localized on the oxygen atoms, and not very far below the δ and δ^* orbitals in energy.

Since two carboxylate groups are present, it is necessary to combine the $p\pi$ orbitals of both into symmetry-adapted linear combinations (SALCs) and then see how they may interact with the δ and δ^* orbitals. The results are shown in Figure 8. The A_u SALC interacts with the δ^* orbital, which has A_u symmetry, pushing it up in energy. The A_g SALC and the δ orbital of B_g symmetry do not interact. Thus, the net effect of the carboxylate groups on the relative energies of the δ and δ^* orbitals is exactly the opposite of that from the μ-Cl atoms, which raise δ relative to δ^*, while the carboxylate group raise δ^* relative to δ.

In summary, the nature of the δ manifold in compounds **1** and **2** is influenced by two factors in addition to the metal–metal bond distance. It remains uncertain which one of these two factors is dominant. Thus we cannot even say with certainty whether the δ level is above or below the δ^* level. The δ orbital of compound **1** may lie higher in energy than the δ^* orbital if the interaction of the δ^* orbital with the $p\pi$ lone-pair orbital on the acetate group is relatively weak, but if this interaction is strong, the δ^* orbital might be even higher than the δ orbital.

A systematic study, in which the ligand environment around the dimolybdenum core is selectively altered, should produce a better understanding of which one of the factors we have discussed is more important in determining M–M distance and singlet–triplet gap. We also plan to perform quantitative calculations.

It is reasonable to think that if the carboxylate groups in compounds **1** and **2** are replaced by the formamidinate groups, the δ^* orbital may be pushed to an energy level higher than π^*, as in the case of $Rh_2(RNCHNR)_4$, $Ru_2(RNNNR)_4$, and $Co_2(RNNNR)_4$, because the energy level of the nonbonding $p\pi$ orbital of a formamidinate group is much higher than that of a carboxylate group and hence it should match better in energy and interact more strongly with δ^*.[9] This reversal of δ^* and π^* in the energy level ordering might well cause the compound $Mo_2Cl_4(tolNCHNtol)_2(PEt_3)_2$ to be completely diamagnetic. Hence, this molecule is a prime synthetic target.

We are aware of the fact that the assumption of the singlet–triplet gap being governed by the δ interactions omits the possibility that antiferromagnetic coupling by a superexchange mechanism might also be involved. It is to be hoped that further work of the sort just outlined will provide a test of the tenability of our assumption.

Comparing compounds **1** and **2**, one can notice that the Mo–Mo distances are almost the same. But for $Mo_2Cl_6(PEt_3)_4$ and $Mo_2Cl_6(PMe_2Ph)_4$,[10,11] the Mo–Mo distances differ by 0.93 Å merely because the phosphines are different. Hence a worthwhile and interesting comparison could be expected if the phosphines in compounds **1** and **2** were replaced by considerably less basic phosphines such as PPh_2Et or PPh_3. Such molecules are therefore also synthetic targets at present.

Acknowledgment. We are grateful to Dr. Maoyu Shang for assistance in the X-ray crystallography and the Texas Advanced Research Program and National Science Foundation for financial support.

Supplementary Material Available: Tables of crystallographic data, bond lengths and angles, and anisotropic thermal parameters and unit cell diagrams for compounds **1** and **2** (11 pages). Ordering information is given on any current masthead page.

(9) Cotton, F. A.; Feng, X. *Inorg. Chem.* **1989**, *28*, 1180.
(10) Poli, R.; Mui, H. D. *Inorg. Chem.* **1989**, *28*, 3609.
(11) Poli, R.; Mui, H. D. *Inorg. Chem.* **1991**, *30*, 65.